Original Paper

To Explore the Mechanism of Atorvastatin Pre-intervention on Cocl2-induced Cardiomyocytes

Zhuomin Wen[1], Limei Liang[2], Jiadong Liang[3], Zhuohua Zhang[4], Cunyu Pan[1], Weijie Zhou[2], Yuxin Jing[1], Guowu Lin[1]

[1] Youjiang Medical University For Nationalities Baise, 533000, Guangxi, China

[2] School of Laboratory Medicine, Youjiang Medical University for Nationalities, China

[3] Clinicopathological Diagnosis and Research Center, Youjiang Medical University for Nationalities Affiliated Hospital, 533000, Guangxi, China

[4] Youjiang Medical University for Nationalities Affiliated Hospital 533000, Guangxi, China

Correspondence: Limei Liang (372549367@qq.com); Weijie Zhou (zhouweijie1998@ymcn.edu.cn)

Abstract

Background: Atorvastatin calcium, known for its anti-inflammatory and atherosclerotic plaque-stabilizing effects, is widely used for the prevention and treatment of ischemic cardiovascular and cerebrovascular diseases, including coronary heart disease, angina pectoris, and cerebral infarction. Pyroptosis, a recently identified form of programmed cell death mediated by Caspase-1 and gasdermin D (GSDMD), is characterized by inflammasome activation and inflammatory cytokine release. Myocardial ischemia/reperfusion injury (MIRI) refers to exacerbated tissue damage that occurs when blood flow is restored (reperfusion) after a transient ischemic episode (insufficient blood supply). Pyroptosis has emerged as a central pathological mechanism in MIRI. In this study, we employed a rat MIRI model and an H9C2 cardiomyocyte hypoxia/reoxygenation (H/R) model to investigate the protective effects and underlying mechanisms of atorvastatin calcium pretreatment in both in vivo and in vitro systems.

Method: In vivo and in vitro models were established using ischemia/reperfusion (I/R) rats and cobalt chloride ($CoCl_2$)-induced hypoxia/reoxygenation (H/R) in H9C2 cells. Cell viability was measured via the CCK-8 assay. The expression levels of pyroptosis-related factors were assessed in both models through Western blotting, RT-qPCR, and immunohistochemical staining.

Result: Nucleotide-binding oligomerization domain (NOD)-like receptor signaling is an important pathway for mediating cardiac inflammation during myocardial I/R. In our experiments, Atorvastatin calcium pretreatment significantly ameliorates I/R-induced myocardial injury and H/R-induced pyroptosis, manifested by improved cardiac histopathology and cell viability. Western blot and RT-qPCR results showed that after pretreatment with atorvastatin calcium, atorvastatin calcium

inhibited the expression of pro-inflammatory cytokines and pyro related molecules, including NLRP3, cleaved caspase-1, and GSDMD.

Conclusion: Our findings suggest that the NOD-like receptor signaling mediated inflammatory plays a pivotal role in myocardial I/R injury. After atorvastatin calcium pretreatment, inflammasome activation and pyroptosis are inhibited by the TLR4/Caspase-1/NLRP3 pathway, thus providing a potential strategy for the treatment of myocardial reperfusion injury.

Introduction

Reperfusion injury is a dynamic process that evolves over a time course ranging from several hours to days (Algoet, Janssens, Himmelreich, et al., 2023). There are growing evidences that reperfusion induces an inflammatory response i in the myocardium (Shen, Wang, Sun, et al., 2022). Therefore, understanding the mechanism of myocardial ischemia-reperfusion injury and exploring therapeutic targets may provide new strategies for the prevention and treatment of myocardial infarction in the future. However, the specific mechanisms by which reperfusion triggers myocardial inflammation remain elusive (Zheng, Xu, Dong, et al., 2022). Atorvastatin calcium, a widely utilized statin in clinical practice, demonstrates a spectrum of cardioprotective effects beyond its lipid-lowering properties (Gao, Jiang, Ge, et al., 2019). Studies have demonstrated that Atorvastatin calcium suppresses cardiomyocyte apoptosis and mitigates I/R injury through concerted mechanisms (Planavila, 2008). Notably, oxidative stress-related targets (Zhang, Qu, Cai, et al., 2024), coupled with signaling pathways implicated in apoptosis and ferroptosis (Sun, Li, & Ji, 2015), have emerged as pivotal pathophysiological nexus underlying the cardioprotective efficacy of Atorvastatin calcium (Yang, Liu, Du, et al., 2021). By systematically interrogating these signaling pathways, researchers are endeavoring to elucidate the multi-layered mechanistic framework that orchestrates the cardioprotective interventional pharmacology of Atorvastatin against I/R injury. We posit that Atorvastatin calcium may exert multimodal regulatory effects on pyroptosis-linked signaling axes, particularly attenuating gasdermin-mediated pyroptotic cascades in the ischemic penumbra to counteract I/R-induced myocardial destabilization. Prior clinical investigations have conclusively demonstrated atorvastatin calcium is beneficial in reducing mortality in patients with cardiovascular disease (Sun, Li, & Ji, 2015; Sun, Liu, Wang, et al., 2024). However, although the mechanism of prevention and action of Ator in I/R has been carefully studied, it still needs to be fully elucidated. The direct evidence between Atorvastatin and pyroptosis in cardiovascular diseases has not yet been elucidated to date. This study aimed to evaluate the effects of Atorvastatin on pyroptosis following MIRI, with a focus on key pyroptosis-related mediators and pathways, including TLR4, NLRP3 inflammasome, caspase-1, and GSDMD. Results demonstrated that Atorvastatin significantly inhibited the expression of these factors in both cobalt chloride-induced hypoxia-reoxygenation models and I/R animal models. Mechanistically, it blocked NLRP3 inflammasome activation, reduced caspase-1 cleavage, and suppressed GSDMD expression and proteolytic processing. These mechanisms collectively suppressed pyroptosis execution,

attenuated myocardial I/R injury, thereby demonstrating substantial cardioprotective effects.

2. Materials and Methods

2.1 Experimental Animals and Cells

Twenty-seven healthy male Sprague-Dawley (SD) rats (6 weeks old, 180-220 g body weight) were obtained from Beijing Vital River Laboratory Animal Technology Co., Ltd. (Animal Facility License: SCXK [Yue] 2022-0063, complying with Guangdong Province laboratory animal regulations). Animals were housed under controlled environmental conditions (temperature: 24 ± 2 ℃, 12-hour light/dark cycle) with ad libitum access to standard rodent chow and water throughout the experimental period. The H9C2 cardiomyocytes used in this experiment were purchased from Wuhan Promai Technology Co., LTD.

2.2 Animal Grouping and Drug Administration

In the experimental animal grouping, 27 healthy Sprague-Dawley (SD) rats were randomly divided into three groups: sham group, ischemia-reperfusion (I/R) group, and treatment group (n=9 per group). Atorvastatin calcium (Ator) was purchased from Jinglepu Medical Technology Co., Ltd. and prepared as a 1 mg/mL suspension. Using dimethyl sulfoxide (DMSO) as a vehicle, the drug was administered via intragastric administration. The treatment group received Atorvastatin calcium solution at a dose of 20 mg/(kg d) for two weeks prior to model establishment, while the sham group and I/R group were administered normal saline, with a total of 14 administrations during this period.

The rats were anesthetized via intraperitoneal injection of pentobarbital sodium (45 mg/kg). Following anesthesia, the surgical procedures were initiated with tracheal intubation and mechanical ventilation using a small animal ventilator. A thoracotomy was performed to expose the heart and coronary arteries. The pericardium was incised between the third and fourth intercostal spaces to fully visualize the cardiac structure. The left anterior descending coronary artery (LAD) was ligated with 6-0 silk suture (sham surgery did not involve ligation) (Xu, Jiang, Yan, et al., 2021).

2.3 Cell Culture and Drug-Induced Cellular Model Establishment

The H9C2 cells were cultured in DMEM medium supplemented with 5% fetal bovine serum (FBS) and 1% penicillin-streptomycin mixture. The culture was maintained in a 37 ℃ incubator with 5% CO_2, and the medium was refreshed every two days. Atorvastatin calcium was prepared as a 1 mg/mL suspension in sterile water, thoroughly dissolved, aliquoted into appropriate containers, and stored frozen. Prior to use, the stock solution was diluted to achieve target concentrations. The H9C2 cell injury model was induced by exposure to 1 mg/mL cobalt chloride ($CoCl_2$).

H9C2 cells in the logarithmic growth phase were uniformly seeded into 10 cm² culture dishes at a density of 130×10^5 cells per dish. To determine the optimal cobalt chloride ($CoCl_2$) concentration for intervention, cells were divided into six experimental groups: blank group, control group, 100 μmol/L $CoCl_2$ group, 200 μmol/L $CoCl_2$ group, 400 μmol/L $CoCl_2$ group, 600 μmol/L $CoCl_2$ group, and 800 μmol/L $CoCl_2$ group. After 18 hours of hypoxia induction, the $CoCl_2$-containing medium was aspirated

and discarded, followed by two washes with phosphate-buffered saline (PBS). Complete culture medium was then added to simulate reoxygenation for 3 hours to identify the optimal $CoCl_2$ concentration. Cell viability was assessed using the CCK-8 assay. Under identical $CoCl_2$ concentrations, cell survival rates were measured at 1 hour, 3 hours, and 5 hours post-reoxygenation following the 18-hour hypoxia period.

2.4 Concentration Screening of Ator

The experiment to screen for the optimal intervention concentration of atorvastatin was divided into 5 groups, with different treatments applied to the cells (Gorji, Alaei-Shahmiri, Darban Hosseini Amirkhiz, et al., 2023). The specific groups were as follows: ① Control group (H9C2 cells treated with normal saline only); ② Cobalt chloride ($CoCl_2$) model group (H9C2 cells treated with 600 μmol/L $CoCl_2$); ③ Low-dose atorvastatin + $CoCl_2$ group (H9C2 cells pretreated with 5 μM atorvastatin for 24 hours, followed by 600 μmol/L $CoCl_2$); ④ Medium-dose atorvastatin + $CoCl_2$ group (H9C2 cells pretreated with 10 μM atorvastatin for 24 hours, followed by 600 μmol/L $CoCl_2$); ⑤ High-dose atorvastatin + $CoCl_2$ group (H9C2 cells pretreated with 20 μM atorvastatin for 24 hours, followed by 600 μmol/L $CoCl_2$). The cells were first pretreated with specified concentrations for 24 hours. Subsequently, the culture medium in the wells was replaced with 600 mmol/L $CoCl_2$ to induce hypoxia for 18 hours. Afterward, the $CoCl_2$ solution was aspirated and discarded, and the cells were washed twice with PBS. Following the addition of complete culture medium to simulate a reoxygenation environment for 3 hours, cell viability was assessed using the CCK-8 assay. The reagent was diluted to working concentration, added to the cells, and incubated in the dark for 1 hour. Absorbance at 450 nm was measured using a microplate reader. The relative cell survival rate was then calculated.

2.5 Quantitative RT-qPCR

Total RNA was extracted from H9C2 cells and myocardial tissues using TRIzol reagent, and RNA concentration was determined by spectrophotometry. Reverse transcription was performed according to the instructions of the reverse transcription kit to obtain cDNA. Subsequently, QRT-PCR amplification of cDNA was conducted using the SYBR Green I PCR kit. A reverse transcription system was established to synthesize cDNA, and a real-time quantitative fluorescence PCR reaction system was prepared. Amplification was performed for 40 cycles under the following conditions using a fluorescence quantitative PCR instrument: 30 sec at 95 ℃, followed by 10 sec at 95 ℃ and 30 sec at 60 ℃. Primer sequences are shown in Table 1. The internal reference gene was β-actin, and the mRNA expression levels of TLR4, caspase-1, and GSDMD were quantified using the $2^{-\Delta\Delta Ct}$ method. Primers for these genes are listed in Table 1.

2.6 Western Blot

Myocardial homogenates were collected from H9C2 cells and myocardial tissues of mice in each group. Total protein was extracted from rat myocardial tissues using RIPA lysis buffer, and protein concentration was measured with a BCA (bicinchoninic acid) protein assay kit. Membranes were incubated with primary antibodies (anti-TLR4, anti-cleaved caspase-1, anti-GSDMD, anti-GAPDH) at

$4\,^{\circ}C$ overnight, followed by incubation with horseradish peroxidase (HRP)-conjugated secondary antibodies at room temperature for 1 hour. Protein signals were visualized using an enhanced chemiluminescence detection system. Band intensity was analyzed using the Image J software.

2.7 Immunohistochemical Staining

Paraffin-embedded tissues were sectioned into 5 μm-thick slices, baked in warm water at $42\,^{\circ}C$, and sequentially immersed in xylene and gradient alcohol solutions for routine dewaxing and rehydration. Sections were then heated in citrate buffer using a microwave oven three times (3 min each) and incubated for 5 min for antigen retrieval. After rinsing, endogenous peroxidase blocker was applied for 10 min, followed by another wash. Goat serum was added for 20 min to block nonspecific binding. After removing the blocking solution, primary antibodies against Caspase-1 (1:250 dilution), GSDMD (1:250), and TLR4 (1:250) were added and incubated overnight. The next day, sections were washed and treated with secondary antibody for 10 min. After thorough rinsing, streptavidin-peroxidase solution was applied for 10 min. Finally, diaminobenzidine (DAB) was used for color development, and nuclei were counterstained with hematoxylin. Under microscopy, Caspase-1-, GSDMD-, and TLR4-positive cells exhibited brown-yellow staining, indicating their expression in myocardial tissues.

2.8 Statistical Analysis

Data were analyzed using GraphPad Prism (8.0.1) and SPSS 26.0 software. Normally distributed measurement data are expressed as mean $\pm$ standard deviation (x $\pm$ s). Analysis of variance (ANOVA) was used for intergroup and intragroup comparisons. Statistical significance was defined as $P < 0.05$ or *$P < 0.01$.

3. Results

3.1 Effect of Cobalt Chloride on H9c2 Cell Viability

Treatment of H9c2 cardiomyocytes with varying concentrations of $CoCl_2$ for 18 hours resulted in a dose-dependent decrease in cell viability. Notably, $CoCl_2$ treatment reduced cell viability by approximately 50%. Significant differences were observed between each concentration group and the control group ($p < 0.05$) (Fig. 1a). At 600 μM $CoCl_2$, cell viability gradually increased after 3 hours of reoxygenation, with a statistically significant difference compared to the control group ($p < 0.05$) (Fig. 1b).

3.2 Effect of Atorvastatin on $CoCl_2$-Induced H9c2 Cell Viability

In vitro experiments showed that 5, 10, 15, and 20 μM atorvastatin had no significant effect on the viability of normal cardiomyocytes (Fig. 2a). Compared to the control group, the H9c2 cell viability in the ischemia-reperfusion (I/R) + low- and medium/high-dose atorvastatin groups increased. The medium-dose atorvastatin in the atorvastatin calcium + $CoCl_2$ treatment group significantly enhanced H9c2 cell viability compared to the H/R group ($P < 0.01$) (Fig. 2b).

3.3 Effect of Atorvastatin on $CoCl_2$-Induced mRNA Levels in H9c2 Cells

To further investigate how atorvastatin calcium reduces TLR4, Caspase-1, and GSDMD mRNA

24

expression, RT-qPCR was performed. Results revealed that the mRNA levels of TLR4, GSDMD, and caspase-1 in the hypoxia-reoxygenation (H/R) model group were significantly increased compared to the control group ($P < 0.01$). Pretreatment with atorvastatin calcium reduced the mRNA expression of TLR4, GSDMD, and Caspase-1 (Fig. 3).

3.4 Atorvastatin Reduces Key Protein Expression in H9c2 Cells

Western blot results demonstrated that the protein expression of TLR4, GSDMD, and caspase-1 in the H/R model group was significantly higher than in the control group ($P < 0.01$). Compared to the H/R model group, pretreatment with atorvastatin decreased the protein levels of TLR4, GSDMD, and caspase-1 in H9c2 cells (Fig. 4).

3.5 Atorvastatin Reduces Key Protein Expression in Animal Tissues

In this study, Western blot analysis was used to examine protein expression in myocardial tissues to determine whether atorvastatin affects myocardial pyroptosis. Compared to the sham group, the I/R group exhibited significantly higher protein levels of TLR4, caspase-1, and GSDMD in myocardial tissues. Atorvastatin effectively reduced the protein levels of TLR4, caspase-1, and GSDMD ($P < 0.05$), consistent with findings from the cellular H/R model (Fig. 5).

3.6 Immunohistochemical Analysis of Inflammatory Factors in Myocardial Tissues After I/R

Immunohistochemical staining revealed an increased number of brown granules in the myocardial tissues of the I/R group compared to the sham group, along with elevated expression levels of TLR4, Caspase-1, and GSDMD. In the pretreatment group, the number of brown granules and the expression levels of TLR4, Caspase-1, and GSDMD in myocardial tissues were reduced compared to the I/R group (Fig. 6).

Table 1.

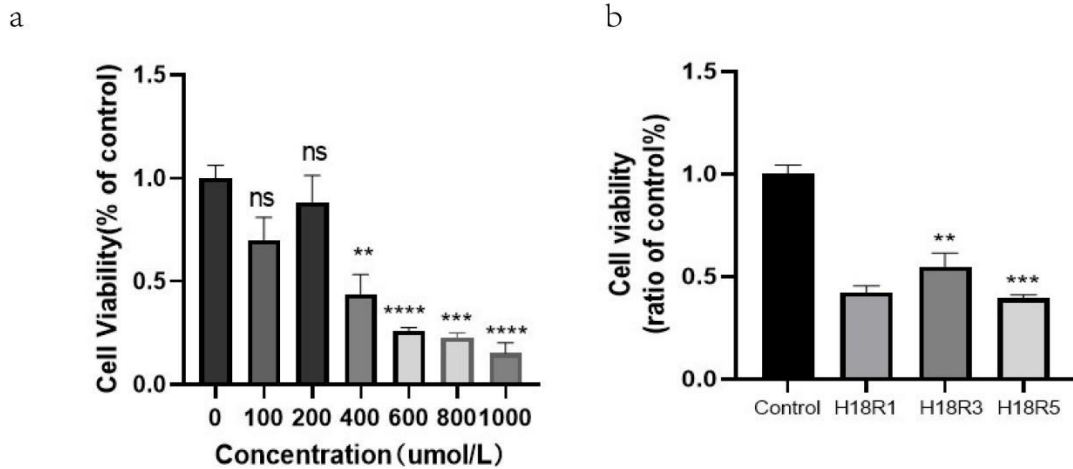| Gene	Primer Type	Primer sequence
TLR4	Forwad	TCGTCATGCTTTCTCACGGC
	Reverse	TCCCAGCCAGATGCAAGAGA
Caspase-1	Forwad	CCGGGCAAGCCAGATGTTTA
	Reverse	GCGCCACCTTCTTTGTTCAG
GSDMD	Forwad	ATCATTGCTCCTCCTGAGCG
	Reverse	CAGCTCAGTAACAGTCCGCC
NLRP3	Forwad	CGAAGCAATGCCCTTGGAGA
	Reverse	GCAGTTGTCTAACTCCAGCA
β-actin	Forwad	ATCATTGCTCCTCCTGAGCG
	Reverse	CAGCTCAGTAACAGTCCGCC

Figure 1. Measurement of cell viability under varying concentrations and reoxygenation durations of cobalt chloride (CoCl₂).

(a) Data are presented as mean ± standard deviation. Statistical significance: *P < 0.01*, **P < 0.001*, and *P < 0.0001*.

(b) Viability of H9c2 cells treated with hypoxia for 18 hours followed by reoxygenation for 1 or 3 hours. Cell viability was measured using the CCK-8 assay. Compared to the control group: **P < 0.01, ***P < 0.001.*
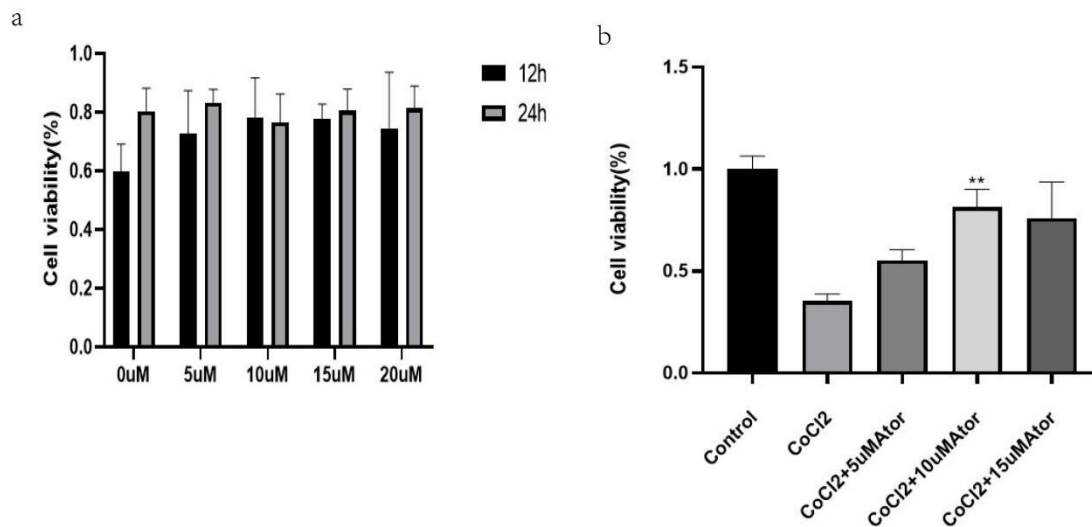

Figure 2. Measurement of cell viability under varying concentrations of atorvastatin calcium.

(a) Effect of 12-hour or 24-hour atorvastatin calcium treatment on H9c2 cell survival rate, assessed using the CCK-8 assay.

(b) Atorvastatin calcium at different concentrations alleviated hypoxia-reoxygenation (H/R)-induced cell death. Cell viability was measured via the CCK-8 assay. Compared to the control group: *** P < 0.01.*
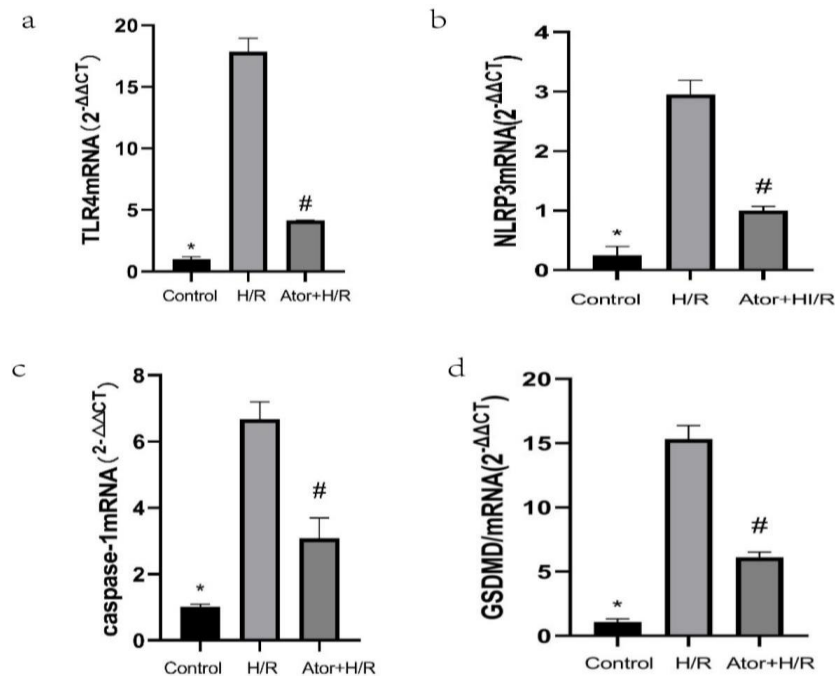
Figure 3. Quantitative analysis of RT-qPCR results, including TLR4, Caspase-1, NLRP3 and GSDMD. All values are expressed as mean ± standard deviation. H/R compared with control group, *P < 0.001; Ator+H/R group compared to H/R group, #P < 0.001.
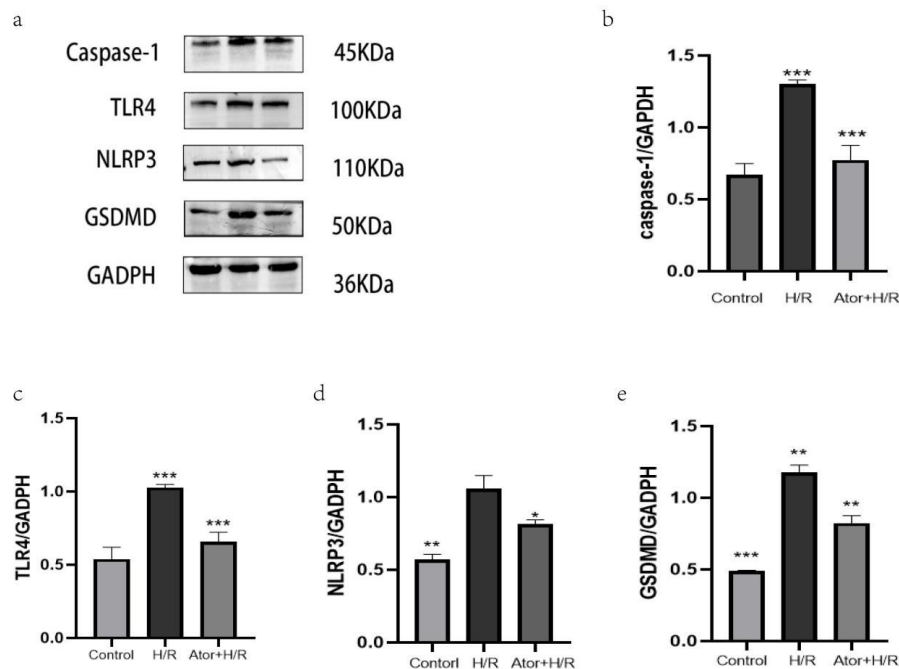

Figure 4. Ator suppresses the activation of TLR4/Caspase-1/NLRP3 in rat H9C2 cells.
(a) Protein levels of cleaved caspase-1, TLR4, NLRP3, and GSDMD in myocardial tissues were evaluated by Western blotting.(b-e) Quantitative analysis of caspase-1, TLR4, NLRP3, and GSDMD protein expression (normalized to GAPDH). Statistical significance: * P < 0:05, ** P < 0:01, and * P < 0:001.
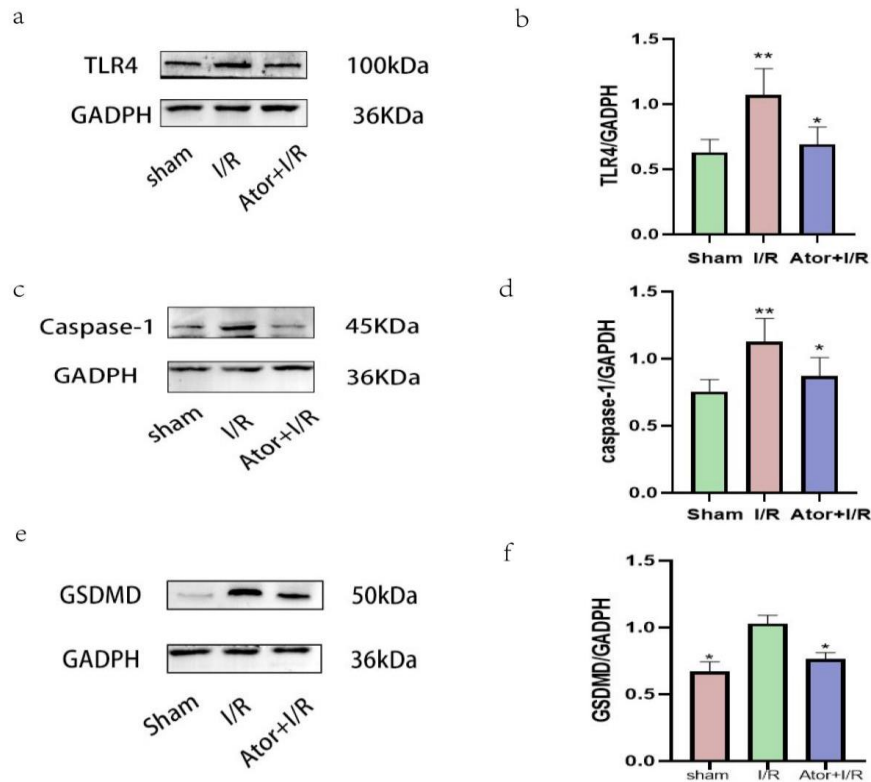
27

Figure 5. Ator suppresses the activation of TLR4/Caspase-1/NLRP3 in rat myocardial tissues. (A and B) Relative expression of TLR4 protein in the Ator pretreatment group. Statistical significance: *P< 0.05, **P<0.01.(C and D) Relative expression of Caspase-1 protein in the Ator pretreatment group.(E and F) Relative expression of GSDMD protein in the Ator pretreatment group.
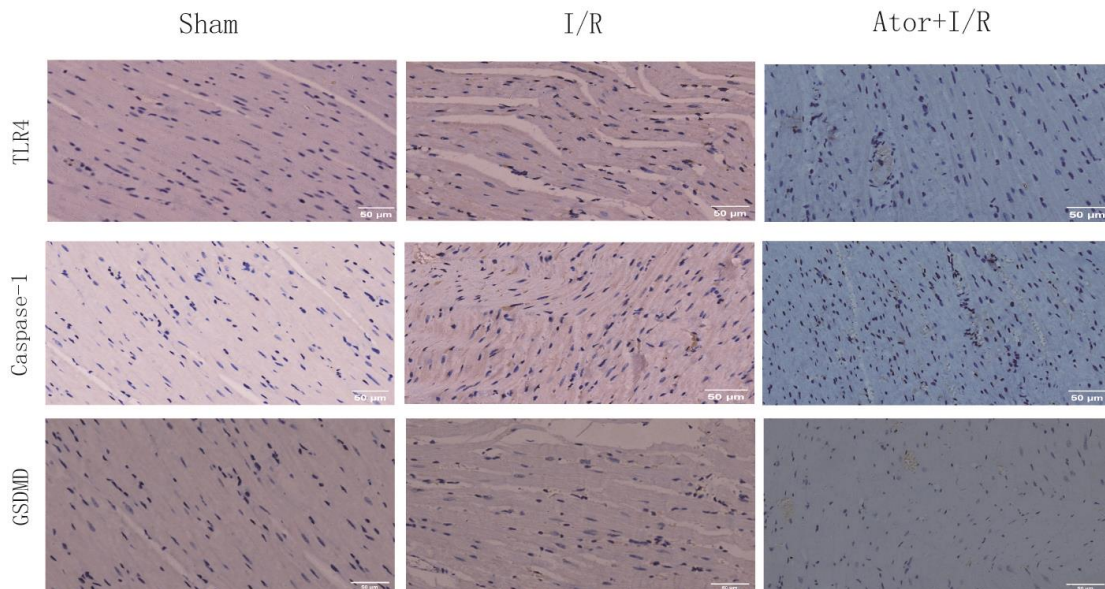

Figure 6. Immunohistochemical images of myocardial tissues in rats from the Sham group, Ischemia/Reperfusion (I/R) group, and Drug Pretreatment group.

28

Discussion

Cardiovascular diseases severely endanger human health, accounting for up to 40% of deaths among urban and rural residents in China (Erdmann, Kessler, Munoz Venegas, et al., 2018; X B, Z W, & J H., 2025). Ischemic heart disease is the primary cause of cardiovascular diseases, leading to reduced myocardial blood supply and insufficient cardiac oxygenation in patients. Acute myocardial infarction, a global ischemic cardiovascular condition, exhibits high mortality and morbidity rates (Pl L, C A, S B, et al., 2022). In recent decades, with the gradual improvement in living standards, the mortality rate of myocardial ischemia has been increasing annually worldwide (Rc, Jk, L, et al., 2024; Martin, Aday, Almarzooq, et al., 2024). Reperfusion therapy serves as an effective treatment for ischemic diseases. However, myocardial reperfusion injury represents a dynamic pathological process that can persist from hours to days while remaining potentially fatal (Tong, Chen, Chen, et al., 2023). Therefore, understanding the mechanisms of myocardial ischemia-reperfusion injury and exploring therapeutic targets may offer new strategies for the future treatment and prevention of myocardial infarction (Zhang, Liu, Hu, et al., 2019).

Pharmacological studies have demonstrated that statins are proven to effectively reduce low-density lipoprotein cholesterol (LDL-C) and prevent atherosclerotic cardiovascular disease (ASCVD) events (S A, Sa B, D K, et al., 2024). Additionally, they can improve vascular endothelial function, inhibit the proliferation and migration of vascular smooth muscle cells, exert antioxidant and anti-inflammatory effects, suppress platelet aggregation, and exhibit antithrombotic properties. These combined effects contribute to preventing atherosclerosis formation/stabilization and reducing cardiovascular risk (Ma, Is, Et, et al., 2023). Previous studies indicate that atorvastatin calcium demonstrates significant therapeutic effects on myocardial ischemia-reperfusion injury (MIRI). Peng et al. (2022) established an MIRI cell model using rat cardiomyocyte H9C2 cells and found that atorvastatin calcium effectively alleviated myocardial cell damage by inhibiting ferroptosis in MIRI injury models. Sun et al. developed an MIRI rat model with SD rats and revealed that atorvastatin calcium alleviates MIRI through the Nrf2 signaling pathway. Hossein Ghaderi-Zefrehi et al. (2024) discovered through human vascular smooth muscle cell lines that atorvastatin calcium exhibits anti-atherosclerotic properties by modulating the ROS-ERK 1/2-Smad 2L signaling pathway. Zhang Xuehui et al. (2022) established a rabbit MIRI model and demonstrated that the combination of pioglitazone and atorvastatin exerts synergistic effects in anti-inflammatory responses and lipid metabolism, further inhibiting atherosclerosis progression and promoting plaque stabilization. Researchers utilizing various cellular and animal experimental models of cardiovascular diseases have consistently shown that atorvastatin calcium possesses both preventive and therapeutic effects, confirming its efficacy in these disease models.

Our study further investigated its potential impact on the pyroptosis pathway. Pyroptosis, a novel form of programmed cell death, typically involves the formation of an inflammasome complex comprising NLRP3, the adaptor protein ASC, and pro-caspase-1 (A P, J P, R L, et al., 2025). Pro-caspase-1 is

29

cleaved by the inflammasome into its active form. Subsequently, active caspase-1 executes two key functions: (1) cleaving GSDMD to promote pore formation in the cell membrane, ultimately leading to cell lysis (Chen, Ying, Zhu, et al., 2025); and (2) processing the precursors IL-1β and IL-18 into their active forms. The release of active IL-1β and IL-18 from cells triggers inflammatory responses (Z W, Y W, F R, et al.).

In this study, we established an *in vitro* myocardial ischemia-reperfusion injury (MIRI) model using cobalt chloride (CoCl₂)-induced hypoxia/reoxygenation (H/R) in H9C2 cardiomyocytes (Yue, Zhang, Zhang, et al., 2024). CCK-8 assay results revealed significant differences in cell viability and morphology between the control and model groups, confirming successful model establishment. Atorvastatin calcium was administered to simulate the MIRI treatment group. Post-treatment with atorvastatin calcium significantly improved H9C2 cell viability, with statistically significant differences observed between the model and treatment groups. These findings suggest that atorvastatin calcium mitigates cardiomyocyte damage. Additionally, in our previous study using an I/R rat model, HE staining demonstrated markedly reduced structural disruption in cardiomyocytes, further validating the cardioprotective effects of atorvastatin calcium (Gong, Lin, Li, et al., 2020).

Following model establishment, we employed Western blotting in both cellular and animal models to investigate the effects of atorvastatin calcium on pyroptosis in MIRI. Results showed significant upregulation of pyroptosis-related proteins TLR4, Caspase-1, NLRP3, and GSDMD in the ischemia-reperfusion (I/R) model. This aligns with prior studies indicating that myocardial I/R injury activates the NLRP3 inflammasome via TLR4 signaling, thereby promoting pyroptosis (Chen, Chen, Zhong, et al., 2021; Chai, Ye, Xue, et al., 2023). Notably, atorvastatin calcium pretreatment significantly suppressed the protein expression levels of these factors. Cellular-level RT-qPCR results further confirmed that atorvastatin calcium markedly inhibited mRNA expression of TLR4, Caspase-1, and GSDMD. These data indicate that atorvastatin calcium reduces NLRP3 inflammasome activation and downstream pyroptosis by inhibiting the TLR4/Caspase-1/NLRP3 signaling axis. This novel finding suggests that the anti-pyroptotic effects of atorvastatin calcium may partially depend on modulation of this signaling pathway, providing new mechanistic insights into its cardioprotective role in MIRI.

This study has several limitations. First, we utilized H/R-treated H9C2 cells rather than primary cardiomyocytes to explore the protective mechanisms of atorvastatin calcium (Del Toro, Licon-Munoz, Crabtree, et al., 2024; Chen, Tian, Wu, et al., 2024). Although the H9C2 rat cardiomyocyte line demonstrates reliability and response consistency, it may not fully replicate the interactions observed in primary cardiomyocytes. Furthermore, the pathophysiology of myocardial I/R injury is complex and may involve factors beyond inflammation, such as oxidative stress and calcium overload (Du, Shi, Xiong, et al., 2022).

Conclusion

In summary, we have demonstrated that atorvastatin calcium effectively protects cardiomyocytes against $CoCl_2$-induced hypoxic injury by inhibiting the TLR4/Caspase-1/NLRP3 signaling pathway. Simultaneously, atorvastatin calcium attenuated myocardial ischemia-reperfusion injury (MIRI) and suppressed NLRP3 inflammasome-mediated pyroptosis. These findings suggest that atorvastatin calcium may serve as a potential prevent agent for combating hypoxic injury in cardiomyocytes.

References

A P, J P, R L, et al. (2025). Resveratrol Reduces Cisplatin-induced Cochlear Hair Cell Pyroptosis by Inhibiting the mtROS/TXNIP/NLRP3 Pathway. *Combinatorial chemistry & high throughput screening*, 2025.

Algoet M, Janssens S, Himmelreich U, et al. (2023). Myocardial ischemia-reperfusion injury and the influence of inflammation. *Trends in Cardiovascular Medicine*, *33*(6), 357-366. https://doi.org/10.1016/j.tcm.2022.02.005

Chai R, Ye Z, Xue W, et al. (2023). Tanshinone IIA inhibits cardiomyocyte pyroptosis through TLR4/NF-κB p65 pathway after acute myocardial infarction. *Frontiers in Cell and Developmental Biology*, *11*, 1252942. https://doi.org/10.3389/fcell.2023.1252942

Chen F, Chen Z Q, Zhong G L, et al. (2021). Nicorandil inhibits TLR4/MyD88/NF-κB/NLRP3 signaling pathway to reduce pyroptosis in rats with myocardial infarction. *Experimental Biology and Medicine (Maywood, N.J.)*, *246*(17), 1938-1947. https://doi.org/10.1177/15353702211013444

Chen J, Tian M, Wu J, et al. (2024). Mesenchymal stem cell conditioned medium improves hypoxic injury to protect islet graft function. Zhong Nan Da Xue Xue Bao. Yi Xue Ban = Journal of Central South University. *Medical Sciences*, *49*(8), 1210-1219.

Chen K, Ying J, Zhu J, et al. (2025). Urolithin A alleviates NLRP3 inflammasome activation and pyroptosis by promoting microglial mitophagy following spinal cord injury. *International Immunopharmacology*, *148*, 114057. https://doi.org/10.1016/j.intimp.2025.114057

Del Toro K, Licon-Munoz Y, Crabtree W, et al. (2024). Breast pericytes: a newly identified driver of tumor cell proliferation. *Frontiers in Oncology*, *14*, 1455484. https://doi.org/10.3389/fonc.2024.1455484

Du S, Shi H, Xiong L, et al. (2022). Canagliflozin mitigates ferroptosis and improves myocardial oxidative stress in mice with diabetic cardiomyopathy. *Frontiers in Endocrinology*, *13*, 1011669. https://doi.org/10.3389/fendo.2022.1011669

Erdmann J, Kessler T, Munoz Venegas L, et al. (2018). A decade of genome-wide association studies for coronary artery disease: the challenges ahead. *Cardiovascular Research*, *114*(9), 1241-1257. https://doi.org/10.1093/cvr/cvy084

Gao G, Jiang S, Ge L, et al. (2019). Atorvastatin Improves Doxorubicin-Induced Cardiac Dysfunction by Modulating Hsp70, Akt, and MAPK Signaling Pathways. *Journal of Cardiovascular*

31

Pharmacology, *73*(4), 223-231. https://doi.org/10.1097/FJC.0000000000000646

Ghaderi-Zefrehi H, Mohammadzadeh G, Rashidi M, et al. (2024). Atorvastatin's Therapeutic Potential in Atherosclerosis: Inhibiting TGF-β-Induced Proteoglycan Glycosaminoglycan Chain Elongation through ROS-ERK1/2-Smad2L Signaling Pathway Modulation in Vascular Smooth Muscle Cells. *Cell Journal*, *26*(2), 158-166.

Gong H J, Lin J J, Li H, et al. (2020). A study on protective effect of morphine against myocardial ischemia-reperfusion injury in rats via CAMP/PKA signaling pathway. *Journal of Biological Regulators and Homeostatic Agents*, *34*(5), 1669-1677. https://doi.org/10.23812/20-224-A

Gorji M T, Alaei-Shahmiri F, Darban Hosseini Amirkhiz G, et al. (2023). Appropriateness of Intensive Statin Treatment in People with Type Two Diabetes and Mild Hypercholesterolemia: A Randomized Clinical Trial. *Archives of Iranian Medicine*, *26*(6), 290-299. https://doi.org/10.34172/aim.2023.45

Ma S, Is M, Et C, et al. (2023). Restoration of normal blood flow in atherosclerotic arteries promotes plaque stabilization. *iScience*, *26*(6). https://doi.org/10.1016/j.isci.2023.106760

Martin S S, Aday A W, Almarzooq Z I, et al. (2024). 2024 Heart Disease and Stroke Statistics: A Report of US and Global Data From the American Heart Association. *Circulation*, *149*(8), e347-e913. https://doi.org/10.1161/CIR.0000000000001247

Peng Y, Liao B, Zhou Y, et al. (2022). Atorvastatin Inhibits Ferroptosis of H9C2 Cells by regulatingSMAD7/Hepcidin Expression to Improve Ischemia-Reperfusion Injury. *Cardiology Research and Practice*, *2022*, 3972829. https://doi.org/10.1155/2022/3972829

Pl L, C A, S B, et al. (2022). The Reduction of Mortality in Acute Myocardial Infarction: From Bed Rest to Future Directions. *International journal of preventive medicine*, *2022*, 13. https://doi.org/10.4103/ijpvm.IJPVM_122_20

Planavila A. (2008). Atorvastatin inhibits GSK-3β phosphorylation by cardiac hypertrophic stimuli. *Biochimica et Biophysica Acta (BBA) - Molecular and Cell Biology of Lipids*, *1781*(1-2), 26-35. https://doi.org/10.1016/j.bbalip.2007.10.009

Rc W, Jk K, L R, et al. (2024). Cardiovascular Disease Mortality Among Native Hawaiian and Pacific Islander Adults Aged 35 Years or Older, 2018 to 2022. *Annals of internal medicine*, *177*(11). https://doi.org/10.7326/M24-0801

S A, Sa B, D K, et al. (2024). Statin Usage in Peripheral Arterial Disease Patients. *The Journal of the Association of Physicians of India*, *72*(6).

Shen S, Wang Z, Sun H, et al. (2022). Role of NLRP3 Inflammasome in Myocardial Ischemia-Reperfusion Injury and Ventricular Remodeling. *Medical Science Monitor: International Medical Journal of Experimental and Clinical Research*, *28*, e934255. https://doi.org/10.12659/MSM.934255

Sun G, Li Y, Ji Z. (2015). Atorvastatin attenuates inflammation and oxidative stress induced by ischemia/reperfusion in rat heart via the Nrf2 transcription factor. *International Journal of Clinical*

and Experimental Medicine, *8*(9), 14837-14845.

Sun X, Liu X, Wang C, et al. (2024). Advantages of statin usage in preventing fractures for men over 50 in the United States: National Health and Nutrition Examination Survey. *PloS One*, *19*(11), e0313583. https://doi.org/10.1371/journal.pone.0313583

Tong G, Chen Y, Chen X, et al. (2023). FGF18 alleviates hepatic ischemia-reperfusion injury via the USP16-mediated KEAP1/Nrf2 signaling pathway in male mice. *Nature Communications*, *14*(1), 6107. https://doi.org/10.1038/s41467-023-41800-x

X B, Z W, J H. (2025). Recent advances in biomimetic nanodelivery systems for the treatment of myocardial ischemia reperfusion injury. *Colloids and surfaces. B, Biointerfaces*, *2025*, 247. https://doi.org/10.1016/j.colsurfb.2024.114414

Xu X na, Jiang Y, Yan L yan, et al. (2021). Aesculin suppresses the NLRP3 inflammasome-mediated pyroptosis via the Akt/GSK3β/NF-κB pathway to mitigate myocardial ischemia/reperfusion injury. *Phytomedicine*, *92*, 153687. https://doi.org/10.1016/j.phymed.2021.153687

Yang H, Liu S, Du H, et al. (2021). Hydrogen Attenuates Myocardial Injury in Rats by Regulating Oxidative Stress and NLRP3 Inflammasome Mediated Pyroptosis. *International Journal of Medical Sciences*, *18*(14), 3318-3325. https://doi.org/10.7150/ijms.61329

Yue Z, Zhang Y, Zhang W, et al. (2024). Kaempferol alleviates myocardial ischemia injury by reducing oxidative stress via the HDAC3-mediated Nrf2 signaling pathway. *Journal of Advanced Research*, *2024*, S2090-1232(24)00491-0. https://doi.org/10.1016/j.jare.2024.10.037

Z W, Y W, F R, et al. (2024). Aloperine Alleviates Atherosclerosis by Inhibiting NLRP3 Inflammasome Activation in Macrophages and ApoE-/- Mice. *Current molecular pharmacology*, *2024*, 17. https://doi.org/10.2174/0118761429342447241214044859

Zhang X, Chen X, Liang Z, et al. (2022). Pioglitazone combined with atorvastatin promotes plaque stabilization in a rabbit model. *Vascular*, *30*(6), 1205-1212. https://doi.org/10.1177/17085381211040992

Zhang Y, Liu D, Hu H, et al. (2019). HIF-1α/BNIP3 signaling pathway-induced-autophagy plays protective role during myocardial ischemia-reperfusion injury. *Biomedicine & Pharmacotherapy = Biomedecine & Pharmacotherapie*, *120*, 109464. https://doi.org/10.1016/j.biopha.2019.109464

Zhang Y, Qu Y, Cai R, et al. (2024). Atorvastatin ameliorates diabetic nephropathy through inhibiting oxidative stress and ferroptosis signaling. *European Journal of Pharmacology*, *976*, 176699. https://doi.org/10.1016/j.ejphar.2024.176699

Zheng Y, Xu L, Dong N, et al. (2022). NLRP3 inflammasome: The rising star in cardiovascular diseases. *Frontiers in Cardiovascular Medicine*, *9*, 927061. https://doi.org/10.3389/fcvm.2022.927061